Density Functional Theory Study of the Properties of N−H···N, Noncooperativities, and Intermolecular Interactions in Linear *trans*-Diazene Clusters up to Ten Molecules

Hua-Jie Song,*,†,‡ He-Ming Xiao,† and Hai-Shan Dong‡

Department of Chemistry, Nanjing University of Science and Technology, Nanjing 210094, China, and Institute of Chemical Materials, China Academy of Engineering Physics, Mianyang 621900, China

Received: February 18, 2006; In Final Form: March 26, 2006

We investigate aspects of N−H···N hydrogen bonding in the linear *trans*-diazene clusters ($n = 2-10$) such as the N···H and N−H lengths, $n(N) \rightarrow \sigma^*(N-H)$ interactions, N···H strengths, and frequencies of the N−H stretching vibrations utilizing the DFT/B3LYP theory, the natural bond orbital (NBO) method, and the theory of atoms in molecules (AIM). Our calculations indicate that the structure and energetics are qualitatively different from the conventional H-bonded systems, which usually exhibit distinct cooperative effects, as cluster size increases. First, a shortening rather than lengthening of the N−H bond is found and thus a blue rather than red shift is predicted. Second, for the title clusters, any sizable cooperative changes in the N−H and N···H lengths, $n(N) \rightarrow \sigma^*(N-H)$ charge transfers, N···H strengths, and frequencies of the N−H stretching vibrations for the linear H-bonded *trans*-diazene clusters do not exist. Because the $n(N) \rightarrow \sigma^*(N-H)$ interaction hardly exhibits cooperative effects, the capability of the linear *trans*-diazene cluster to localize electrons at the N···H bond critical point is almost independent of cluster size and thereby leads to the noncooperative changes in the N···H lengths and strengths and the N−H stretching frequencies. Third, the dispersion energy is sizable and important; more than 30% of short-range dispersion energy not being reproduced by the DFT leads to the underestimation of the interaction energies by DFT/B3LYP. The calculated nonadditive interaction energies show that, unlike the conventional H-boned systems, the *trans*-diazene clusters indeed exhibit very weak nonadditive interactions.

1. Introduction

The importance of hydrogen bonding has been recognized in a wide range of chemical and biophysical phenomena. Most H-bonded A−H···B systems exhibit so-called cooperative effects which reflect in marked contraction in the B···H bonds (or elongation of the A−H bonds) and an obvious red shift of the A−H stretching frequencies.[1−7] However, in contrast to the general H-bonded systems, the linear *trans*-diazene clusters considered here hardly have the obvious cooperative effects.

Diazene (HN═NH) is an important chemical compound which is used in the selective reduction of nonpolar bonds[8] and as ligands in transition metal complexes.[9] It is also the parent substance of azo compounds. Diazene has therefore been the subject of numerous investigations, both experimental[10−16] and theoretical.[17−24] Almost all of the computations reported indicated that of the three isomers of N_2H_2 (cis, trans, and iso), the trans-form is the most stable and the energy ordering is trans < cis < iso.[17−19,21−24] As a matter of fact, only the trans-isomer has been observed so far in the gas phase.[25] The experimental evidence for *cis*-diazene is more sparse. Very little is known about the third isomer of diazene, namely, *iso*-diazene (H_2N═N), in which both hydrogens are attached to the same nitrogen.

Although the molecule diazene (N_2H_2) has been the subject of many theoretical studies, the investigations on the properties and interactions of diazene clusters have not been done from survey. Therefore, experimental measurements provide no detailed structural information about the structure of the clusters involved or the characteristics of the interaction. One must use theoretical methods to derive it. In this work, we investigate aspects of the H···N H-bonds (HBs) and the nature of the noncooperativities in the linear *trans*-diazene clusters.

2. Theoretical Methods

Full geometry optimization and vibration analysis of the linear *trans*-diazene clusters ($n = 2-10$) which are bound via the N···H bonds have been performed at the B3LYP/6-31++G** level with the Gaussian03 program.[26] The interaction energies of the optimized clusters are evaluated at the B3LYP/aug-cc-pvdz level using the supermolecule approach (SM)[27] where interaction energy is calculated as a subtraction of the energy of a cluster by a sum of the full supermolecule basis set energies of its monomers at the geometries adopting in the cluster. The basis set superposition errors (BSSEs) of these SM interaction energies (E_{int}^{SM}) have been corrected utilizing the counterpoise technique.[28]

The natural bond orbital (NBO) method corresponds closely to the picture of localized bonds and lone pairs as basic units of molecular structure.[29] According to the NBO method, the shift of electron density as a result of H-bond formation can be identified by comparing the charges of the individual atoms in the uncomplexed and complexed states. Unlike Mulliken or other charge partitioning schemes, the NBO scheme is unaffected by the presence of diffuse functions in the basis set adopted here.[29] The NBO method provides a useful tool for exploring the nature of the HBs.[1,2,29] On the other hand, Bader's theory of atoms in molecules (AIM)[30] has been widely used in

* To whom correspondence should be addressed. E-mail: hjsongmoru@tom.com.

† Nanjing University of Science and Technology.

‡ China Academy of Engineering Physics.

10.1021/jp061053r CCC: $33.50
Published on Web 04/18/2006

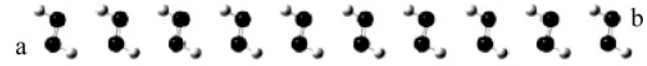

Figure 1. Optimized geometry for the decamer. A rule about labeling atoms of the clusters ($n = 2-10$) is also given. For example, H(2a) means the H atom on unit 2 in chain "a", N(8b) stands for the N atom on unit 8 in chain "b". The black balls represent N atoms; the white balls represent H atoms.

TABLE 1: Lengths of N−H Bonds R_{N-H} (Å) and Charge Transfers at Size $n = 10$

R_{N-H}[a]		unit	q_{HB} (10^{-4} e)	q_{CT} (10^{-4} e)
N(1a)−H(1a)	**1.0372**	1	−8.1	−8.4
N(2a)−H(2a)	**1.0367**	2	6.1	6.7
N(3a)−H(3a)	**1.0366**	3	2.2	1.9
N(4a)−H(4a)	**1.0366**	4	0.1	0.2
N(5a)−H(5a)	**1.0366**	5	−0.3	−0.3
N(6a)−H(6a)	**1.0366**	6	−0.3	−0.3
N(7a)−H(7a)	**1.0367**	7	0.1	0.2
N(8a)−H(8a)	**1.0365**	8	2.2	1.9,
N(9a)−H(9a)	**1.0364**	9	6.1	6.7
N(10a)−H(10a)	1.0360	10	−8.1	−8.3

[a] Since the clusters are C_{2h} symmetries, only the R_{N-H} values of chain "a" are listed; the N−H bonds acting as H-donors are displayed in bold.

investigating or characterizing the properties at the HB bond critical points (BCPs).[1,31−37]

We employ the DFT, NBO, and AIM theories to study the optimized geometries, charge transfers, N···H strengths, and N−H IR spectra of *trans*-diazene clusters up to 10 molecules and look at the origin of the noncooperativities in the clusters.

3. Results and Discussion

3.1. Lengths of the N−H and N···H bonds. Although not imposing any symmetries during the geometrical optimizations, all of the optimal *trans*-diazene clusters ($n = 1-10$) have linear open chain structures with C_{2h} symmetries (within the tolerance of 0.01), as shown in Figure 1. High-resolution IR spectroscopy gave evidence for the C_{2h} symmetry of the *trans*-diazene molecule.[11,12] For its isolated molecule, N−N = 0.1244 nm, N−H = 0.1036 nm, and H−N−N = 106.8°, which are in reasonable agreement with the experimentally deduced geometry for the *trans*-isomer (N−N = 0.1252 nm, N−H = 0.1028 nm, and H−N−N = 106.9°).[11] Here, we focus only upon the N−H and N···H lengths at $n = 2-10$. The lengths for the decamer ($n = 10$) are listed in Tables 1 and 2, respectively.

All of the N−H bonds acting as H-donors are almost elongated relative to the N−H length of the isolated *trans*-diazene molecule (0.10363 nm). However, the magnitude of the elongation in chain "a" for each cluster gradually diminishes from the left unit to the right unit. The same is also true of chain "b", progressively from right to left. On the other hand, the N−H bond on unit 1 (viz., the left terminal unit) of chain "b" (N(1b) −H(1b)) and that on unit *n* (viz., the right terminal unit) of chain "a" (N(*n*a)−H(*n*a)) are not H-donors and hence shorter than 0.10363 nm. In this way, the N−H length at each cluster size *n* progressively decreases from the left unit to the right unit along chain "a" (or from the left unit to the right unit along chain "b"). Therefore, the magnitude of the decrease in N−H length can be expressed by a difference between the N−H lengths of unit 1 and unit *n* in chain "a". The difference values are given as follows: 0.00100 nm for the dimer, 0.00118 nm for the trimer, 0.00126 nm for the tetramer, 0.00135 nm for the pentamer, 0.00136 nm for the hexamer, 0.00117 nm for the heptamer, 0.00126 nm for the octamer, 0.00123 nm for the enneamer, and 0.00122 nm for the decamer. We did not find any marked change with cluster size from these values. Among the "H-donor" N−H bonds at size $n > 2$, the elongations relative to the length of N(1a)−H(1a) or N(2b)−H(2b) of the dimer (0.10370 nm) are only found in N(1a)−H(1a) and N(*n*b)−H(*n*b) (viz, N(b)−H(b) of the right terminal unit). As a matter of fact, the elongations are less than 3×10^{-5} nm and thus can be neglected. Unexpectedly, there are slight shrinkages relative to the value of 0.10370 nm in the "H-donor" N−H bonds on the interior units of the cluster chains, reflecting that the slight changes are contrary to the cooperative effects existing in most H-bonded systems. The average lengths of the N−H bonds on the interior units per cluster for $n = 3-10$ are 0.10364, 0.10365, 0.10365, 0.10365, 0.10365, 0.10366, 0.10365, and 0.10366 nm, respectively. Both geometries for the "H-donor" N−H bonds on the terminal units and those on the interior units change hardly with cluster size. Therefore, there is no cooperative change in the N−H bonds as cluster size increases.

TABLE 2: N···H Lengths $R_{N\cdots H}$ (Å), Actual Charge Transfers ($q_{n\to\sigma^*}$) along the HBs (10^{-3} au), Stabilization Energies $E^{(2)}_{n(N)\to\sigma^*}$ (kJ/mol), Electron Densities $\rho(\mathbf{r}_{cp})$ (10^{-2} au) and Their Laplacian $\nabla^2\rho(\mathbf{r}_{cp})$ (10^{-2} au), and Local Electronic Potential Energy Density (kilojoules per mole per atomic unit volume) of the 90 N···H Bonds at Size $n = 10$

HB[a]	$R_{N\cdots H}$	$q_{n\to\sigma^*}$	$E^{(2)}_{n(N)\to\sigma^*}$	$\rho(\mathbf{r}_{cp})$	$\nabla^2\rho(\mathbf{r}_{cp})$	$V_A(\mathbf{r}_{cp})$	$V(\mathbf{r}_{cp})$
1a···2a	2.2816	8.29	19.372	1.631	4.083	−24.754	-26.781
9b···10b	2.2816	8.29	19.372	1.631	4.084	−24.756	-26.782
2a···3a	2.2745	8.31	19.414	1.656	4.160	−25.326	-27.261
8b···9b	2.2745	8.31	19.414	1.656	4.160	−25.328	-27.263
3a···4a	2.2763	8.25	19.288	1.650	4.143	−25.183	-27.156
7b···8b	2.2763	8.25	19.288	1.650	4.143	−25.185	-27.157
4a···5a	2.2766	8.24	19.246	1.649	4.140	−25.160	-27.136
6b···7b	2.2765	8.24	19.246	1.649	4.140	−25.162	-27.137
5a···6a	2.2762	8.25	19.288	1.650	4.143	−25.184	-27.151
5b···6b	2.2762	8.25	19.288	1.650	4.143	−25.186	-27.153
6a···7a	2.2756	8.27	19.330	1.651	4.148	−25.220	-27.176
4b···5b	2.2756	8.27	19.330	1.651	4.148	−25.222	-27.177
7a···8a	2.2755	8.27	19.330	1.651	4.150	−25.222	-27.178
3b···4b	2.2755	8.27	19.330	1.651	4.150	−25.223	-27.178
8a···9a	2.2773	8.11	19.163	1.644	4.135	−25.075	-27.068
2b···3b	2.2773	8.11	19.163	1.644	4.135	−25.076	-27.069
9a···10a	2.2865	7.48	17.866	1.611	4.048	−24.347	-26.459
1b···2b	2.2865	7.48	17.866	1.611	4.048	−24.349	-26.460

[a] In this column, the labels of the N and H atoms of the N···H bonds that are given in Figure 1 are listed.

The average N···H length per cluster is as follows: 0.2296 nm for the dimer, 0.2286 nm for the trimer, 0.2283 nm for the tetramer, 0.2281 nm for the pentamer, 0.2280 nm for the hexamer, 0.2280 nm for the heptamer, 0.2279 nm for the octamer, 0.2278 nm for the enneamer, and 0.2278 nm for the decamer. Unlike most H-bonded systems, the contraction in N···H does not enhance conspicuously with cluster size.

It has been reported[1−4] that, for most A−H···B systems, an obvious contraction in H···B (or elongation in A−H) with increased size of H-bonded systems is pervasive, which is regarded as an important signature of the cooperative effects in these systems. Different from the H-bonded systems, however, the linear *trans*-diazane clusters almost do not have cooperative effects in the geometric sense.

3.2. Vibrational Frequencies of the N-H Bonds. It has been extensively reported[1−4] that red shifts of the A−H stretching frequencies in the A−H···B systems generally increase with the H-bonded cluster size; this is a reflection of cooperative effects. Therefore, the displacement in the hydride stretching frequency is always an indicator of the nature of cooperativity.

On the basis of the vibrational analysis of the optimized linear *trans*-diazane clusters at the B3LYP/6-31++G** level, the

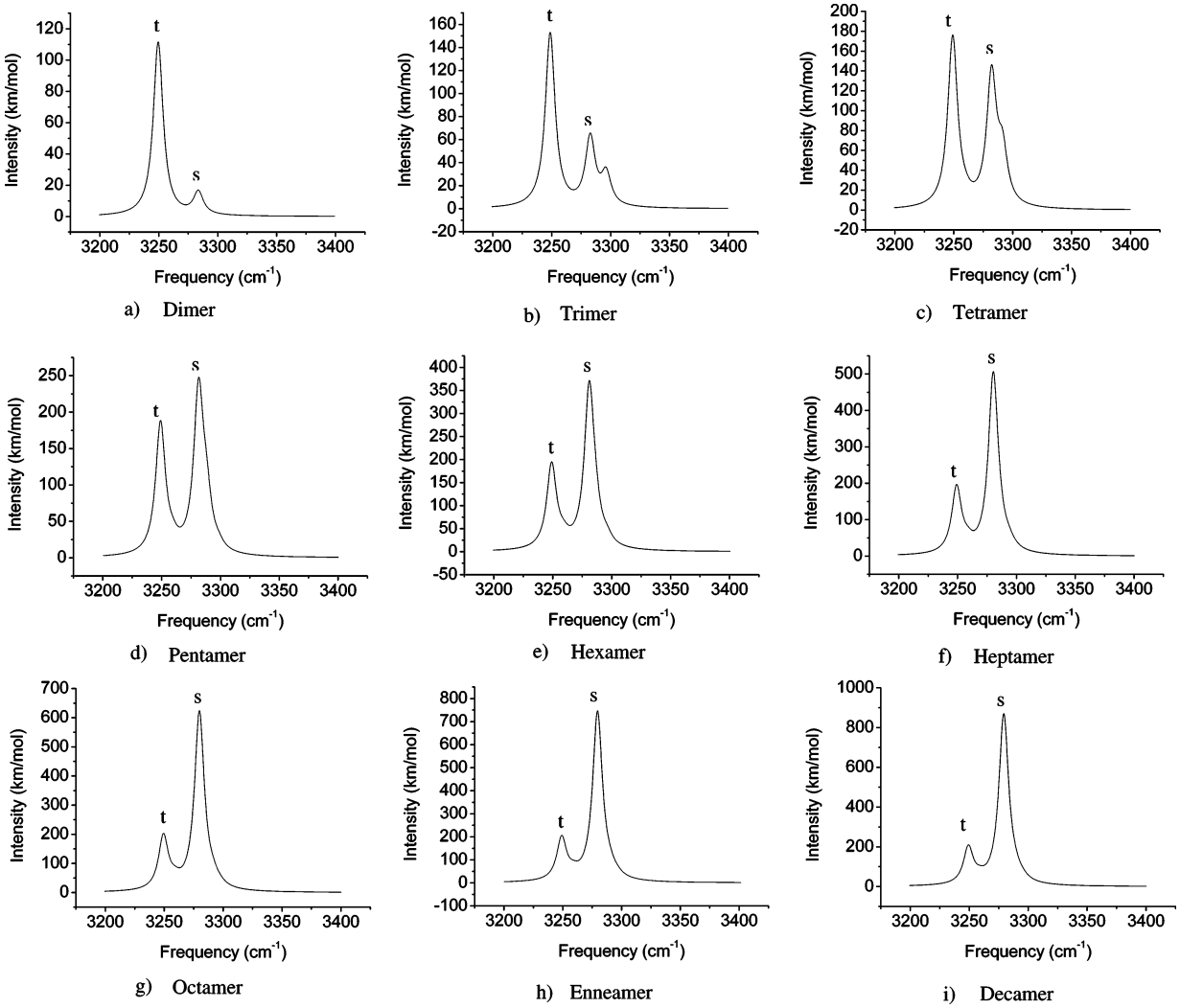

Figure 2. IR spectra of the N−H stretching vibrations at $n = 2-10$.

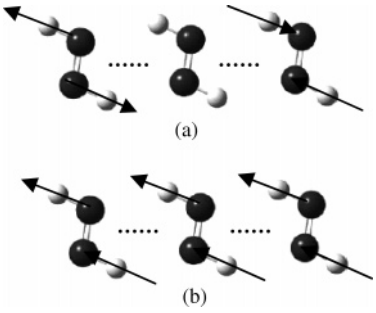

Figure 3. Two important normal modes of N−H stretching vibrations: (a) "t" normal mode and (b) "s" normal mode. The black balls represent N atoms; the white balls represent H atoms.

N−H vibrational spectra of these clusters ($n = 2-10$) are plotted in Figure 2. Among the N−H normal stretching modes for each cluster, two important modes that are graphically displayed in Figure 3 are observed: one is combined by the N−H stretches on two terminal monomer units, which is shown in Figure 3a; the other is synthesized by the stretches on all monomer units, which is shown in Figure 3b. In this article, "t" stands for the former mode, "s" for the latter. For each cluster, the IR intensities of the "s" and "t" modes are always strongest among all of the N−H stretching modes. Table 3 gives the stretching frequencies of the two modes (ν_t and ν_s). The frequency of the "t" mode is always lowest among the N−H vibration modes in each of the clusters.

TABLE 3: Dipole Moments μ (Debye) and Vibrational Frequencies (cm^{-1}) at $n = 2-10$

n	μ	ν_t	ν_s
2	0.0004	3249.54	3283.61
3	0.0008	3248.76	3282.76
4	0.0009	3249.13	3282.13
5	0.0001	3249.02	3281.44
6	0.0006	3249.06	3280.98
7	0.0007	3249.13	3280.33
8	0.0012	3249.36	3279.86
9	0.0008	3249.02	3279.57
10	0.0003	3249.26	3279.3

For the isolated *trans*-diazane molecule, only two N−H stretching modes exist in its N−H IR spectrum. One locates at 3248.56 cm^{-1}, and its intensity is 0.0084 km/mol; the other is at 3278.27 cm^{-1}, and its intensity is 33.4979 km/mol. The former mode (H ← N═N → H) corresponds to the "t" mode, and the latter (H ← N═N ← H) corresponds to the "s" mode. According to Table 3, frequency shifts of the "t" modes for the clusters ($n = 2-10$) are less than 1 cm^{-1} relative to 3248.56 cm^{-1}. The frequency displacement of the "t" modes is almost invariant to cluster size. When cluster size is up to 5, the intensity of this mode arrives at a saturation value of about 180 km/mol. Clearly, the "t" mode does not take on a cooperative change at all. On the other hand, although the intensities of the "s" modes increase markedly with cluster size, their frequencies are blue shifted as compared with the corresponding frequency

of 3278.27 cm^{-1} of the isolated molecule. This is very different from most A−H···B systems where the A−H stretching frequencies are always red shifted relative to their isolated molecules.[1−4] On the other hand, it has been widely reported[38−42] that the frequency blue shift of the H-donor bond is known to happen in so-called "anti-hydrogen" bonds (the shortening and the blue shift of the proton donor A−H) like the C−H···π, C−H···O, and C−H···X (X = halogen) improper, blue-shifting H-bonds. However, as mentioned in section 3.1, the "H-donor" N−H bonds are slightly elongated rather than shortened relative to the isolated molecule (0.10363 nm). Hence, the H···N does not completely meet the two requirements of the "anti-hydrogen" bond. In this way, it is conjectured that the blue shift observed in the "s" modes may not be attributed to the two-step mechanism[38,39] for the "anti-hydrogen" bond. Since the lengths of the N(1b)−H(1b) and N(*n*a)−H(*n*a) bonds at size *n* that are not proton donors are shortened as compared with 0.10363 nm, the vibrations of the non-H-donor bonds promote the "s" mode to blue shift. And the H-donors N−H vibrations should try to force the mode to red shift. Clearly, the ability of the former vibrations to blue shift the "s" mode is substantially superior to the ability of the latter vibrations to red shift it. Expressed another way, the potential ability of red shift in the H-donor N−H bonds is very weak, indicating that the "H-donor" bonds hardly have conspicuous cooperativities. We also note that the magnitude of the blue shift lessens slightly with cluster size. This may be attributed to a slight enhancement in the ability to red shift the "s" mode as cluster size increases. However, the enhancement does not thoroughly reverse the blue shift trend of the "s" mode. In a word, the change in the N−H stretching frequencies with cluster size indicates that the cooperative effects of the linear systems are very weak.

3.3. Role of the *n*(N) → σ*(N−H) Interactions. In terms of the NBO theory,[29] A−H···B bonding can be attributed to the localized *n*(B) → σ*(A−H) interaction, that is, electronic delocalization from the filled lone pair *n*(B) of the "electron donor" B into the unfilled antibond σ*(A−H) of the "electron acceptor" A−H. According to ref 29, we estimate the actual charge-transfer quantities ($q_{n\to\sigma^*}$) due to the *n*(N) → σ*(N−H) interactions at the B3LYP/aug-cc-pvdz level and thus derive the net charge-transfer quantities (q_{HB}) along the N···H bonds. In principle, the shift in electron density rather than being localized over a particular region delocalizes throughout the acceptor and donor molecules. Therefore, the net charges (q_{CT}) distributed over the monomer units due to the shifts in electron densities are also evaluated. The q_{HB} and q_{CT} values for the linear decamer are collected in Table 1. As can clearly be seen, the net charges on the two terminal units are always negative and the charges on the interior units are almost positive. A good linear correlation between q_{HB} and q_{CT} can be expressed by

$$q_{HB} = 0.92 q_{CT} \qquad (1)$$

Thereby, the correlation expression indicates that the *n*(N) → σ*(N−H) interactions play decisive roles in the charge transfers. Since the clusters have C_{2h} symmetries, the *n*(N) → σ*(N−H) interactions along chain "a" and chain "b" nearly counteract each other and thus their dipole moments μ (see Table 3) almost vanish. This is exactly why the net charges q_{CT} on the monomers are less than 10^{-3} au, judging from the average values of $q_{n\to\sigma^*}$ per cluster at *n* = 2−10 that are 0.00754, 0.00785, 0.00786, 0.00804, 0.00809, 0.00813, 0.00814, 0.00817, and 0.00816 au, respectively. No cooperative change in charge transfers with cluster size is observed in the *trans*-diazene clusters, which are sharply contrasted with the conspicuously cooperative change in charge transfers existing in most H-bonded systems.[1−4]

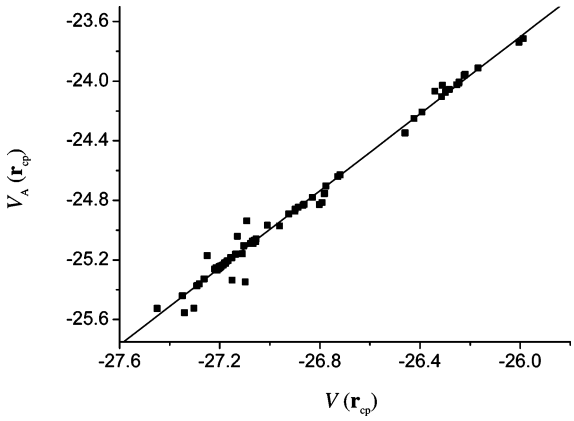

Figure 4. $V_A(\mathbf{r}_{cp})$ vs $V(\mathbf{r}_{cp})$ values at the critical points of 90 N···H bonds. Units are in kilojoules per mole per atomic unit volume. The solid line corresponds to the linear fit: $V_A(\mathbf{r}_{cp}) = 9.90 + 1.29V(\mathbf{r}_{cp})$, with the correlation factor being 0.995.

The stabilization energy $E^{(2)}_{n(N)\to\sigma^*}$ as a consequence of the *n*(N) → σ*(N−H) interaction reflects the attractive interaction in the N···H bonding and thus can be used to characterize the strength of the N···H bond. According to ref 29, we have computed the energies for the clusters at the B3LYP/aug-cc-pvdz level. The estimated $E^{(2)}_{n(N)\to\sigma^*}$ data for the decamer along with the $q_{n\to\sigma^*}$ values are listed in Table 2. Recently, it has been reported[1] that because of strong cooperative effects in the linear $(cis\text{-}N_3H_3)_n$ clusters, the average value of $E^{(2)}_{n(N)\to\sigma^*}$ at size *n* = 8 more than doubles the average at *n* = 2. The estimated average values of $E^{(2)}_{n(N)\to\sigma^*}$ per monomer for the *trans*-diazene clusters (*n* = 2−10) are 17.824, 17.928, 18.477, 18.786, 18.933, 19.016, 19.079, 19.146, and 19.116 kJ/mol, respectively. The average at *n* = 10 is only 1.07 times that for the dimer, illustrating that the stabilization energies of the linear *trans*-diazene clusters almost do not exhibit the pronounced cooperative effects.

3.4. Strengths of the N···H Bonds. In terms of Espinosal's proposal,[32,35] the local electronic potential energy density ($V(\mathbf{r}_{cp})$) can represent the capacity of the *trans*-diazene cluster in concentrating electrons at the N···H BCP and provides an approach to describing the N···H strength. We have calculated $\rho(\mathbf{r}_{cp})$, $\nabla^2\rho(\mathbf{r}_{cp})$, and $V(\mathbf{r}_{cp})$ of the 90 N···H bonds from the topological analysis of the B3LYP/aug-cc-pvdz electron densities of the equilibrium clusters (*n* = 2−10) with the AIM2000 program.[43] In addition, Abramov has proposed the evaluation of the local electronic potential energy density from the experimental electron density distribution.[32,34,36,45] The Abramov's local electronic potential energy density $V_A(\mathbf{r}_{cp})$ can be evaluated according to the following expression[32,34,36]

$$V_A(\mathbf{r}_{cp}) = -\left(\frac{3}{5}(3\pi^2)^{2/3}\rho^{5/3}(\mathbf{r}_{cp}) + \frac{1}{12}\nabla^2\rho(\mathbf{r}_{cp})\right) \qquad (2)$$

Table 2 gives the $\rho(\mathbf{r}_{cp})$, $\nabla^2\rho(\mathbf{r}_{cp})$, $V(\mathbf{r}_{cp})$, and $V_A(\mathbf{r}_{cp})$ values at size *n* = 10. The positive $\nabla^2\rho(\mathbf{r}_{cp})$ is of the same order of magnitude as $\rho(\mathbf{r}_{cp})$ ($\sim 10^{-2}$ au), indicating that the 90 N···H bonds have the general characteristics of the H-bond that have been pointed out by many studies.[44] Figure 4 compares the calculated values of $V_A(\mathbf{r}_{cp})$ from eq 2 with the $V(\mathbf{r}_{cp})$ data from the topological analysis for the 90 N···H bonds. The distribution of the points exhibits a very good linear relationship between $V(\mathbf{r}_{cp})$ and $V_A(\mathbf{r}_{cp})$. The graphical representation indicates that eq 2 can equivalently evaluate the capacity of the *trans*-diazene

cluster in concentrating electrons at the N···H BCP and the N···H strength.

The estimated average values of $V_A(\mathbf{r}_{cp})$ per cluster for $n = 2-10$ are −23.727, −24.229, −24.696, −24.856, −24.956, −25.017, −25.028, −25.059, and −25.090 kJ/mol, respectively. Clearly, the average value of $V_A(\mathbf{r}_{cp})$ for the decamer is only 1.06 times that for the dimer. Thus, it can be concluded that the capacity of the *trans*-diazene cluster to concentrate electrons at the N···H BCP does not enhance with cluster size. The conclusion is completely the same as that drawn from $E^{(2)}_{n(N)\rightarrow\sigma^*}$. In fact, according to $E^{(2)}_{n(N)\rightarrow\sigma^*}$ and $V_A(\mathbf{r}_{cp})$ of the 90 HBs, a crude linear relation between the two physical quantities is observed

$$V_A(\mathbf{r}_{cp}) = -(11.54 + 0.704E^{(2)}_{n(N)\rightarrow\sigma^*}) \quad (3)$$

The correlation shows that the two representations of the N···H strengths based upon NBO and AIM are approximately equivalent.

Thereby, we believe that, because the $n(N) \rightarrow \sigma^*(N-H)$ interaction hardly takes on cooperativity, the capacity of the linear *trans*-diazene cluster to concentrate electrons at the N···H BCP is almost insensitive to the cluster size, as is also reflected in the fact that the average value of $\rho(\mathbf{r}_{cp})$ (0.01645) for the decamer is only 1.04 times that for the dimer (0.01580 au).

3.5. Interaction Energies. It has been well-known that DFT fails to describe the dispersion bound systems.[46−49] Since the hydrogen-bonded complex is dominated by electrostatic and inductive interactions, many DFT functionals have been found capable of describing the complex to a reasonably good accuracy.[50,51] Recently, however, we reported[52] that, although the H-bonded linear *cis*,*trans*-cyclotriazane (N_3H_3) dimer is dominated by electrostatic and inductive interactions, the DFT/B3LYP was found unable to yield satisfactory interaction energy due to the fact that about 40% of the short-range dispersion energy is neglected by the DFT.

According to the SAPT(DFT) method,[52−56] a combination of symmetry-adapted perturbation theory (SAPT)[57] with asymptotically corrected DFT, we have estimated the electrostatic energy (−37.134 kJ/mol), the induction energy (−10.851 kJ/mol), the dispersion energy with exchange-dispersion effect (−13.543 kJ/mol), and the repulsion energy (39.823 kJ/mol) of the *trans*-diazene dimer utilizing the aug-cc-pvdz basis set. The calculated interaction energies at the B3LYP, MP2, and MP4/aug-cc-pvdz levels using the supermolecular approach (SM) are −17.398, −21.466, and −20.706 kJ/mol, respectively. Clearly, the sum of the electrostatic and induction energies has a great capability to overcome the repulsion. The H-bonded dimer is essentially electrostatic in nature like the conventional H-bonded systems. However, the electrostatic picture of the H-bond does not necessarily prove that no other interactions are important in N···H hydrogen bonding. We also notice that the dispersion energy (−13.543 kJ/mol), over 65% of the MP4 interaction energy, is sizable and important. On the other hand, the accuracy of the MP2 energy is very good when compared with the MP4 energy, but the B3LYP interaction energy $E^{SM(B3LYP)}_{int}$ accounting for only about 81% of the MP2 energy does not yield a satisfactory accuracy. Since B3LYP has a good ability to account for the classic electrostatic, induction, and exchange components,[52] we can estimate the part of the dispersion reproduced by B3LYP for the dimer, which is about −9.24 kJ/mol, only 66% of the dispersion energy (−13.90 kJ/mol) contained in the correlation part of the MP2 interaction energy. Clearly, B3LYP reproduces partially the dispersion at short-range distances. This is exactly why the DFT fails to yield satisfactory interaction energy.

TABLE 4: Calculated Interaction Energies (kJ/mol) for the *trans*-diazene Clusters ($n = 2-10$) at the B3LYP/aug-cc-pvdz Level

cluster size	$E^{SM(B3LYP)}_{int}$	ΔE_{Add}	E^{C}_{int}	$E^{SM(MP2)}_{int}$	E_{NA} (B3LYP)
2	−17.398	−4.068	−21.466	−21.466	0
3	−35.541	−8.427	−43.968	−43.995	−0.449
4	−53.759	−12.787	−66.546	−66.661	−0.869
5	−72.063	−17.201	−89.264	−89.367	−1.254
6	−90.334	−21.558	−111.892		−1.641
7	−108.603	−25.984	−134.587		−2.026
8	−126.878	−30.398	−157.276		−2.291
9	−145.150	−34.778	−179.927		−2.802
10	−163.422	−39.159	−202.581		−3.172

Since the clusters have very weak nonadditive interactions, the part of dispersion energy neglected by DFT/B3LYP can be regarded as a quantity of approximate pair additivity. We have calculated the combined interaction energy of molecular pairs at the MP2/aug-cc-pvdz level (E_{Add}(MP2)), that is, the sum of the interaction energies of all the dimers in each cluster. Thus, the additive dispersion energy (ΔE_{Add}) neglected by DFT/B3LYP can be evaluated by

$$\Delta E_{Add} = E_{Add}(MP2) - E_{Add}(B3LYP) \quad (6)$$

where E_{Add}(B3LYP) is for the combined interaction energy of molecular pairs at the B3LYP/aug-cc-pvdz level. On the basis of ΔE_{Add}, $E^{SM(B3LYP)}_{int}$ can be corrected by

$$E^{C}_{int} = E^{SM(B3LYP)}_{int} + \Delta E_{Add} \quad (7)$$

$E^{SM(B3LYP)}_{int}$, ΔE_{Add}, and E^{C}_{int} are listed in Table 4. For these clusters, ΔE_{Add} accounts for ∼19% of E^{C}_{int}, thereby the deficiency of B3LYP in reproducing the short-range dispersion indeed is responsible for the underestimation of the B3LYP interaction energies. The canonical MP2 interaction energies $E^{SM(MP2)}_{int}$ for the trimer, tetramer, and pentamer have also been computed and are listed in Table 4. The $|E^{C}_{int}/E^{SM(MP2)}_{int} - 1| \times 100\%$ values for them are less than 0.2%, showing that this correction can arrive at a very high accuracy.

The nonadditive energy is calculated as the difference between the combined interaction energy of molecular pairs and the interaction energy of the complex. The nonadditive energies (E_{NA}(B3LYP)) of these clusters at the B3LYP/aug-cc-pvdz levels are also collected in Table 4. The E_{NA}(B3LYP) values are less than 1.6% of E^{C}_{int}, and the nonadditive energies hardly increase with cluster size, indicating that the noncooperativity in the $n(N) \rightarrow \sigma^*(N-H)$ interaction indeed leads to the vanishing nonadditive energy.

4. Summary and Conclusions

We have employed reasonably the DFT/B3LYP, NBO, and AIM theories to investigate aspects of N−H···N hydrogen bonding in linear H-bonded *trans*-diazene clusters ($n = 2-10$), such as N···H and N−H lengths, $n(N) \rightarrow \sigma^*(N-H)$ interactions, HB strengths, and frequencies of N−H stretching vibrations. Our calculations indicate that, as cluster size increases, any obvious cooperative changes in the N−H and N···H lengths, $n(N) \rightarrow \sigma^*(N-H)$ interactions (charge transfers), strengths of the N···H bonds, and frequencies of the N−H stretching vibrations almost are not found, which is very different from

the conventional H-bonded systems where there are conspicuous cooperative changes in the corresponding properties. The linear H-bonded *trans*-diazene clusters seem to be exceptions to conventional H-bonded systems.

We also observe that the two representations of N···H strengths based upon NBO and AIM can be regarded as approximately equivalent. Because the $n(\mathrm{N}) \rightarrow \sigma^*(\mathrm{N-H})$ interactions hardly take on cooperative effects, the capacity of the linear *trans*-diazene cluster to concentrate electrons at the N···H BCP is almost invariant to cluster size, thereby leading to the noncooperative changes in the N···H lengths and strengths and the N−H stretching frequencies.

More than 30% of short-range dispersion energy not being reproduced by the DFT leads to the failure of the DFT/B3LYP to estimate successfully the interaction energies for the linear clusters. The corrected DFT/B3LYP interaction energies arrive at a high accuracy. The calculated nonadditive energies E_{NA}(B3LYP) of these clusters are less than 1.6% of the corrected B3LYP interaction energies, showing that the *trans*-diazene clusters unlike most H-bonded systems have very weak nonadditive interactions.

Acknowledgment. This work is research project 42101030410 of the Institute of Chemical Materials and also supported by the National Natural Science Foundation of China (Grant No. 20173028) and the fund of CAEP (No. 2002Z0501).

Supporting Information Available: Tables giving computational data about the $R_{\mathrm{N-H}}$ and $R_{\mathrm{N\cdots H}}$, $q_{n\rightarrow\sigma^*}$, q_{HB}, q_{CT}, $E_{n(\mathrm{N})\rightarrow\sigma^*}{}^{(2)}$ $\rho(\mathbf{r}_{\mathrm{cp}})$, $\nabla^2\rho(\mathbf{r}_{\mathrm{cp}})$, $V_{\mathrm{A}}(\mathbf{r}_{\mathrm{cp}})$, and $V(\mathbf{r}_{\mathrm{cp}})$ values at sizes $n = 2-10$ and Cartesian coordinates of optimized geometries as well as the complete ref 26. This material is available free of charge via the Internet at http://pubs.acs.org.

References and Notes

(1) Song, H.-J.; Xiao, H.-M.; Dong, H.-S.; Zhu, W.-H. *J. Phys. Chem. A* **2006**, *110*, 2225−2230.
(2) King, B. F.; Weinhold, F. *J. Chem. Phys.* **1995**, *103*, 333−347.
(3) Cabaleiro-Lago, E. M.; Ríos, M. A. *J. Phys. Chem. A* **1999**, *103*, 6468−6474.
(4) Mandado, M.; Graña, A. M.; Mosquera, R. A. *Chem. Phys. Lett.* **2003**, *381*, 22−29.
(5) Huyskens, P. L. *J. Am. Chem. Soc.* **1977**, *99*, 2578−2582.
(6) Kleeberg, H.; Klein, D.; Luck, W. A. P. *J. Phys. Chem.* **1987**, *91*, 3200−3203.
(7) Maes, G.; Smets, J. *J. Phys. Chem.* **1993**, *97*, 1818−1825.
(8) Vidyarthi, S. K.; Willis, C.; Back, R. A.; Mcittrick, R. M. *J. Am. Chem. Soc.* **1974**, *96*, 7647−7650.
(9) Veith, M. *Angew. Chem., Int. Ed. Engl.* **1976**, *15*, 387−388.
(10) Rosengren, K.; Pimentel, G. C. *J. Chem. Phys.* **1965**, *43*, 507−516.
(11) Carlotti, M.; Johns, J. W. C.; Trombetti, A. *Can. J. Phys.* **1974**, *52*, 340−344.
(12) Craig, N. C.; Levin, I. W. *J. Chem. Phys.* **1979**, *71*, 400−407.
(13) Wiberg, N.; Fisher, G.; Bachhuber, H. *Angew. Chem., Int. Ed. Engl.* **1977**, *16*, 780−782.
(14) Sylwester, A. P.; Dervan, P. O. *J. Am. Chem. Soc.* **1984**, *106*, 4648−4650.
(15) Biehl, H.; Stuhl, F. *J. Chem. Phys.* **1994**, *100*, 141−145.
(16) Demasion, J.; Hegelund, F.; Bürger, H. *J. Mol. Struct.* **1997**, *413*, 447−456.
(17) Jensen, H. J. A.; Jørgensen, P.; Helgaker, T. *J. Am. Chem. Soc.* **1987**, *109*, 2895−2910.
(18) Pople, J. A.; Curtiss, L. A. *J. Chem. Phys.* **1991**, *95*, 4385−4388.
(19) Walch, S. P. *J. Chem. Phys.* **1989**, *91*, 389−394.
(20) Smith, B. J. *J. Phys. Chem.* **1993**, *97*, 10513−10514.
(21) Goldberg, N.; Holthausen, M. C.; Hrušák, J.; Koch, W.; Schwarz, H. *Chem. Ber.* **1993**, *126*, 2753−2758.
(22) Andzelm, J.; Sosa, C.; Eades, R. A. *J. Phys. Chem.* **1993**, *97*, 4664−4669.
(23) Angeli, C.; Cimiraglia, R.; Höfmann, H.-J. *Chem. Phys. Lett.* **1996**, *259*, 276−282.
(24) Jursić, B. *Chem. Phys. Lett.* **1996**, *261*, 13−17 and references therein.
(25) Foner, S. N.; Hudson, R. L. *J. Chem. Phys.* **1958**, *28*, 719−720.
(26) Frisch, M. J.; et al. *Gaussian 03*, revision B.05; Gaussian, Inc.: Pittsburgh, PA, 2003.
(27) Chałasinski, G.; Szczesniak, M. M. *Chem. Rev.* **2000**, *100*, 4227−4252.
(28) Boys, S. F.; Bernardi, F. *Mol. Phys.* **1970**, *19*, 553−559.
(29) Reed, A. E.; Curtiss, L. A.; Weinhold, F. *Chem. Rev.* **1988**, *88*, 899−926.
(30) Bader, R. F. W. *Acc. Chem. Res.* **1985**, *18*, 9−15.
(31) Koch, U.; Popelier, P. L. A. *J. Phys. Chem.* **1995**, *99*, 9747−9754.
(32) Espinosa, E.; Molins, E.; Lecomte, C. *Chem. Phys. Lett.* **1998**, *285*, 170−173.
(33) Espinosa, E.; Southassou, M.; Lachekar, H.; Lecomte, C. *Acta Crystallogr., Sect. B: Struct. Sci.* **1999**, *55*, 563−572.
(34) Espinosa, E.; Lecomte, C.; Molins, E. *Chem. Phys. Lett.* **1999**, *300*, 745−748.
(35) Espinosa, E.; Molins, E. *J. Chem. Phys.* **2000**, *113*, 5686−5694.
(36) Espinosa, E.; Alkorta, I.; Rozas, I.; Elguero, J.; Molins, E. *Chem. Phys. Lett.* **2001**, *336*, 457−461.
(37) Espinosa, E.; Alkorta, I.; Elguero, J.; Molins, E. *J. Chem. Phys.* **2002**, *117*, 5529−5542.
(38) Hobza, P.; Havlas, Z. *Chem Rev.* **2000**, *100*, 4253−4264 and references therein.
(39) van der Velen, B. J.; Herrebout, W. A.; Szostak, R.; Shchepkin, D. N.; Havlas, Z.; Hobza, P. *J. Am. Chem. Soc.* **2001**, *123*, 12290−3.
(40) Zierkiewicz, W.; Michalska, D.; Havlas, Z.; Hobza, P. *ChemPhysChem* **2002**, *3*, 511−518.
(41) Reimann, B.; Buchhold, K.; Vaupel, S.; Brutschy, B.; Havlas, Z.; Špirko, V.; Hobza, P. *J. Am. Chem. Soc.* **2002**, *124*, 11854−11855.
(42) Delanoye, S. N.; Herrebout, W. A.; van der Veken, B. J. *J. Am. Chem. Soc.* **2002**, *124*, 11854−11855.
(43) Biegler-König, F.; Schönbohm, J.; Bayles, D. *J. Comput. Chem.* **2001**, *22*, 545−559.
(44) Bone, R. G. A.; Bader, R. R W. *J. Phys. Chem.* **1996**, *100*, 10892−10911 and references therein.
(45) Abramov, Y. A. *Acta Crystallogr., Sect. A: Found. Crystallogr.* **1997**, *53*, 264−272.
(46) Kristyan, S.; Pulay, P. *Chem. Phys. Lett.* **1994**, *229*, 175−180.
(47) Perez-Jorda, J.; Becke, A. D. *Chem. Phys. Lett.* **1995**, *233*, 134−137.
(48) Perez-Jorda, J.; San-Fabiaan, E.; Perez-Jimenez, A. *J. Chem. Phys.* **1999**, *110*, 1916−1920.
(49) Meijer, E. J.; Sprik, M. *J. Chem. Phys.* **1996**, *105*, 8684−8689.
(50) Tsuzuki, S.; Lüthi, H. P. *J. Chem. Phys.* **2001**, *114*, 3949−3967.
(51) Tuma, C.; Boese, A. D.; Handy, N. C. *Phys. Chem. Chem. Phys.* **1999**, *1*, 3939−3947.
(52) Song, H.-J.; Xiao, H.-M.; Dong, H.-S. Dong *J. Chem. Phys.* **2006**, *124*, 074317−10.
(53) Williams, H. L.; Chabalowski, C. F. *J. Phys. Chem. A* **2001**, *105*, 646−659.
(54) Song, H.-J.; Xiao, H.-M.; Dong, H.-S. *Sci. China, Ser. B: Chem.* **2004**, *47*, 466−479.
(55) Misquitta, A. J.; Szalewicz, K. *J. Chem. Phys.* **2005**, *122*, 214109−19.
(56) Misquitta, A. J.; Podeszwa, R.; Jeziorski, B.; Szalewicz, K. *J. Chem. Phys.* **2005**, *123*, 214103−14.
(57) Jeziorski, B.; Moszynski, R.; Szalewicz, K. *Chem. Rev.* **1994**, *94*, 1887.